Journal of Applied Electrochemistry **33**: 135–142, 2003.

Unusual cavity shapes resulting from multistep mass transport controlled dissolution: Numerical simulation and experimental investigation with titanium using oxide film laser lithography

P.-F. CHAUVY and D. LANDOLT*
Institute of Materials – LMCH, Swiss Federal Institute of Technology Lausanne, CH-1015 Lausanne EPFL, Switzerland
*(*author for correspondence, fax: +41 21 693 39 46, e-mail: dieter.landolt@epfl.ch)*

Received 19 August 2002; accepted in revised form 10 October 2002

Key words: electrochemical micromachining, isotropic etching, pitting corrosion, shape evolution, titanium

Abstract

The shape evolution of cavities produced by multistep electrochemical micromachining is investigated both theoretically and experimentally. A boundary element code is used for 2D simulation of the shape evolution as a function of applied charge. A two-step process is simulated by assuming that metal dissolves from a small area at the bottom of a hemicylindrical groove protected by an insulating film. Similarly, the shape evolution in a three-step process is numerically simulated. The simulation shows that multistep isotropic etching can yield buried cavities with a narrow opening as well as large aspect ratio cavities. It also permits one to achieve aspect ratios larger than one. Electrochemical micromachining experiments were carried out with titanium using oxide film laser lithography (OFLL) for patterning the surface. Metal dissolution from the irradiated line features on the oxide was carried out in an electropolishing electrolyte starting from a flat surface or from preformed grooves. The resulting cavity shapes observed with a microscope corresponded well to the theoretical predictions. The experiments thus confirmed that isotropic etching involving two or three subsequent anodization–irradiation–dissolution steps can yield high aspect ratio cavities and partly occluded cavities. Possible implications of the present results for the shape evolution of corrosion pits are discussed.

1. Introduction

Electrochemical micromachining (EMM) is a relatively recent microfabrication process for shaping and surface structuring of metals [1–8]. In EMM a photoresist is irradiated through a mask to create a pattern and the exposed metal is then anodically dissolved in a suitable electrolyte. The shape evolution of a dissolving individual feature has been studied by several authors both experimentally and theoretically [2, 6, 9, 10]. For mass transport controlled isotropic etching cavities of hemicylindrical or hemispherical shape were obtained after sufficiently long dissolution times [2, 6]. An important quantity is the so called etch factor which characterizes the widening of the dissolving cavity due to undercutting in relation to the cavity depth. Using theoretical simulation West et al. [2] showed that for a mass transport controlled dissolution process the values of the etch factor for a linear groove and hemispherical feature are very close. Therefore, 2D simulation considering the cross section of a groove is a good approximation for the study of the shape evolution of hemispherical features. Madore et al. [6] studied the application of EMM to surface microstructuring of titanium using a sulfuric acid–methanol electrolyte originally developed for electropolishing [11]. Isotropic etching with smooth surface finish resulted from dissolution under mass transport control [6]. More recently, it was found that an anodically formed oxide film can assume the role of the photoresist [12]. Based on that observation a maskless micromachining process for titanium was developed using selective laser irradiation of an oxide film covered metal surface to form a pattern [13, 14]. The use of oxide film laser lithography (OFLL) permits patterning of on nonplanar surfaces and the fabrication of multilevel structures [14]. Electrochemical micromachining of multilevel structures using conventional photoresist techniques is relatively limited, as discussed by Ferri et al. [8]. Laser oxide film lithography facilitates multistep etching because several consecutive anodization–irradiation–dissolution steps can be applied to a sample. The feasibility of the technique has been demonstrated by Chauvy et al. [14] who fabricated a two level model microstructure for microfluidics applications. In their technique the microstructured surface formed in a first irradiation–oxidation–dissolution step

was re-anodized and then again selectively irradiated. Dissolution of the irradiated features yielded the second level microstructure. In principle, the described processing sequence can be repeated to produce three-level or multilevel structures.

Pitting corrosion involves the spontaneous formation of cavities on a passive metal surface due to local passive film breakdown. Several authors found that pit growth under certain conditions occurs in the presence of a salt film at the pit bottom and the growth rate is controlled by mass transport of the dissolution away from the pit surface [15–19]. Few theoretical studies on the shape evolution of corrosion pits have been published. According to Vetter and Stehblow hemispherical electropolished pits are formed in the presence of salt films [15]. Actual corrosion pits are rarely hemispherical, however, occluded shapes or deep pits being more common. Newman and coworkers recently [20, 22, 23] proposed that pits in stainless steel grow from a hemispherical nucleus by a salt film transport mechanism. Open pits have a hemispherical shape, but more often a lacy cover forms by undercutting which leads to formation of occluded pits and a flattening of the pit shape. Theoretical models for the formation of occluded pits have been proposed by Laycock et al. [24, 25]. Wang et al. [21] studied the shape of model pits with a narrow neck for nickel in a sulfuric acid solution. These authors explained the formation of a neck by repassivation due to the *IR* drop in the electrolyte. However, only upwards facing cavities exhibited a characteristic shape with a neck indicating that convection may also have played a role in their experiments.

The goal of the present study is to investigate experimentally and by numerical simulation the shape evolution of cavities subjected to multistep isotropic etching. Of particular interest is the formation of buried cavities with a neck and of high aspect ratio cavities. The theoretical predictions were verified using titanium, because previous studies have shown that anodic etching of titanium in electropolishing electrolytes is mass transport controlled [11]. To facilitate the preparation of cross sections grooves rather than pits were studied.

2. Experimental method

Electrochemical micromachining (EMM) based on oxide film laser lithography has been described elsewhere in detail [13, 14, 26]. It involves four steps (Figure 1): anodic oxidation of the metal, selective laser irradiation of the oxide covered surface, electrochemical dissolution of the metal from the exposed features, ultrasonic cleaning. The first step involves the anodic oxidation of a mirror finished titanium surface in 0.5 M aqueous sulfuric acid. A high rate (20 V s^{-1}) potential sweep is applied in a two-electrode set-up using a platinum counter electrode. For optimum results on mechanically polished surfaces the voltage is swept to 100 V and on electropolished surfaces to 40 V. The oxide-covered samples are then locally irradiated in air using a XeCl excimer laser (model LPX 300 from Lambda Physics, wave length 308 nm, pulse length 20 ns). An energy attenuator allows for precise setting of the fluence. A computer controlled beam shutter together with x–y tables permits automated writing through a Labview interface. A simple mask projection optical system is used to define the pattern. The mask consists of a square aperture 100 μm × 100 μm laser-machined in a 50 μm thick molybdenum foil. A fused silica convergent lens ($f = 100$ mm) projects the image of the mask onto the sample. Distances between the elements are set to ensure a reduction factor of 10 between the mask and the projected image. A single laser pulse of 1000 mJ cm^{-2} was found sufficient to locally sensitize the titanium oxide surface. The interactions between the laser beam and the oxide film covered titanium surfaces under these conditions are complex and will be discussed elsewhere

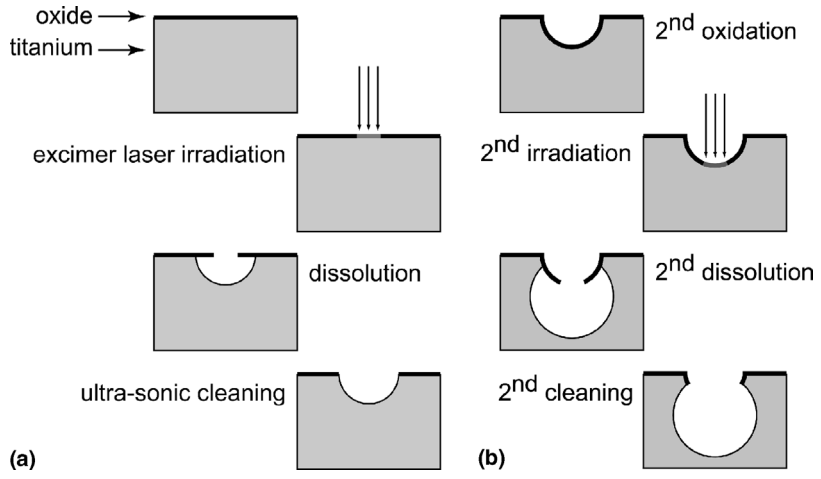

Fig. 1. Schematic of oxide film laser lithography process for producing a one-level cavity (a) and a two-level cavity (b) by electrochemical micromachining.

in detail [27]. Lines are written by scanning the sample perpendicular to the laser beam at a speed of 400 μm s^{-1} and a laser pulse repetition rate of 80 Hz.

For multilevel micromachining a precise positioning system is needed because lithography and dissolution are carried out in separate set-ups. A small specially designed digital optical microscope was used for this purpose including a simple lens ($f = 12$ mm) and a small digital camera (Conrad Electronic GmbH, CCD Fingerkamera). Images are displayed on a TV screen. The view on the screen corresponds to a sample area of 100 μm $\times$ 150 μm. The microscope is positioned 5 cm beside the laser irradiation spot. Reference marks are written by laser irradiation and the image of the marks is stored. Prior to further irradiation the sample marks are aligned with the stored image to achieve micrometer precision positioning.

Electrochemical dissolution is carried out at −10 °C in an electropolishing electrolyte containing 3 M sulfuric acid in methanol [3]. Potentiodynamic control is applied in a two-electrode set-up (circular titanium counter-electrode) in the following sequence: 20 V for 20 s, then decrease to 10 V in 10 s and maintaining 10 V until the desired charge has been passed. Under the experimental conditions the dissolution process is mass transport limited and therefore isotropic in nature [6]. The charge necessary to create a predefined microstructure is calculated on a volumetric basis using Faraday's law and a valence of 4 [11].

Figure 1(b) shows the principle of adding a second oxidation–irradiation–dissolution step on a hemicylindrical groove. After micromachining of the first level, the titanium surface is anodically oxidised (40 V) and a second laser irradiation is performed in the centre at the bottom of the groove. A second etching step is then carried out and a new cavity is formed within the old one. An ultrasonic cleaning step is again required to neatly break the underetched oxide. Three-level microstructures were realised using the same procedure by adding a third oxidation–irradiation–dissolution step. The precision in the positioning of the laser beam is on the order of a few μm. The good precision of the positioning system is illustrated by the SEM picture of Figure 2(a) which shows a laser written line at the bottom of a previously etched groove. The SEM picture of Figure 2(b) shows the same geometrical feature after anodic dissolution.

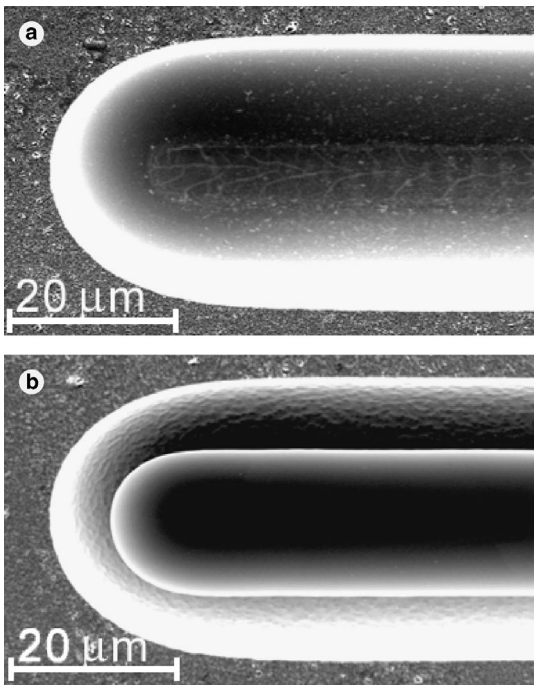

Fig. 2. (a) Laser trace at the bottom of a groove illustrating the good precision of the alignment of the beam. (b) Same groove after etching of the second level.

3. Numerical simulation

Numerical simulations were carried out to predict the cavity shape resulting from multistep isotropic etching of line shapes. The length of the etched grooves was assumed to be much larger than their width, so a 2D geometry could be used to simulate the shape evolution of the cross section. Because isotropic etching leads to symmetrical cross section profiles, the calculations were performed for single half grooves only. The numerical approach used for the simulation was the same as described by Madore et al. [6]. A moving boundary simulation was used where at each time step the current distribution along the metal surface is calculated. The calculation of the current distribution of a diffusion-limited reaction is mathematically identical to the calculation of a primary current distribution. Laplace's equation for concentration was therefore used with constant concentration boundary conditions. For the present system the concentration of dissolving metal ions at the metal surface is equal to the saturation concentration whereas the concentration at the outer boundary is zero. Laplace's equation was solved at each step by the LAPLACE code written in Fortran 77. Between each step additional programs were used to calculate the new profile position and to add boundary nodes in order to ensure a constant point density (2 pts μm^{-1}). Displacement is set in a way that between each step the point at $x = 0$ is moved across a specified distance (0.1 μm). The outer boundary was assumed to correspond to the outer edge of a Nernst diffusion layer of constant thickness. This geometry was used for simplicity; the results obtained showed no significant differences compared to simulations with an outer boundary of hemicylindrical shape used previously [6].

Cavity shapes were calculated for a laser spot diameter of 10 μm. The irradiation was assumed to create a trace of same width in the oxide film. One level etching simulations were started from a flat surface. Etching of second level cavities was assumed to start from an initial 20 μm deep quasi-hemicircular cavity at the bottom of which a 10 μm wide trace was produced by laser irradiation. The three-level simulations assumed dissolution

to start from an irradiated second level cavity of 40 μm depth. Figure 3 presents the results of the numerical simulations. Figure 3(a) shows the shape evolution of a cavity formed in a one step process. For small charges it exhibits a flat-bottomed shape, slightly higher in the centre than near the edges. This shape reflects the fact that in the initial phase the diffusion rate at the edge is higher than in the centre [2, 10]. With increasing dissolution the effect disappears and the cross section assumes an almost hemicircular shape. The data of Figure 3(a) are in good agreement with previously reported results for cylindrical and spherical cavities [2, 6]. Figure 3(b) shows the simulated shape evolution of a cavity formed in a two-step process. It is assumed that in a first step a hemicylindrical cavity of 40 μm diameter has been formed. Its surface is covered by an insulating film except for a 10 μm diameter trace in the centre. From that spot the metal dissolves anodically under mass transport control, while the remainder of the film stays in place.

The shape evolution as a function of applied charge shown in the figure indicates that the initial geometry of the second level cavity resembles that of a first level cavity exhibiting a centre surface slightly higher than that near the edges (Figure 3(a)). However, as the dissolution proceeds the cavity deepens and the effect disappears. A second level cavity shape with an inner diameter larger than the opening is formed. Eventually, the shape of the first level cavity is no longer perceived; a large cavity is

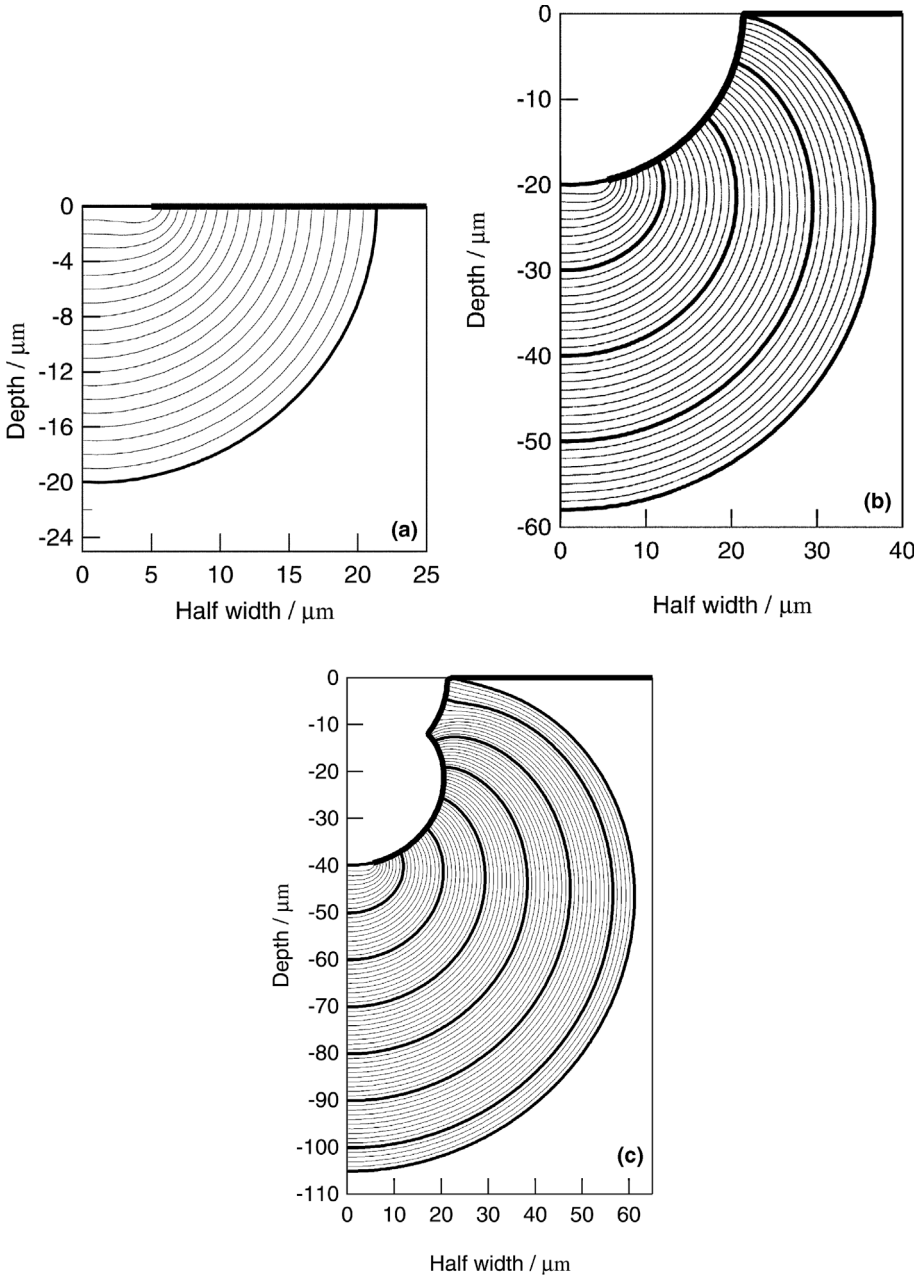

Fig. 3. Simulated shape changes resulting from diffusion controlled dissolution at different applied charge. (a) Cavity etched from a flat surface, (b) two-level cavity, (c) three-level cavity. Thick line represents the insulating oxide film.

formed with an opening that is narrower than the inner cavity diameter. In Figure 3(c) a shape change simulation involving three oxidation–irradiation–dissolution steps is shown. The hemicircular 40 μm deep second level cavity is covered by an insulating film except for a centre spot of 10 μm. Anodic dissolution of the exposed area leads to formation of a third level cavity, which grows, with applied charge. At first the shape of all three cavities can be clearly distinguished, and the overall shape corresponds to a much higher aspect ratio than can be achieved by single step isotropic etching. With increasing dissolution time the second and third level cavities increasingly merge into a wide bottomed deep cavity with a neck. Finally, all three cavities merge, yielding a large regularly shaped cavity with an ever shorter neck that finally disappears. The original multilevel cavities can no longer be distinguished in this case.

4. Results

To test the model predictions experiments were carried out with titanium using laser lithography. Microstructures consisting of an array of 10 parallel lines 4 mm long and 100 μm apart were fabricated using oxide film laser lithography. Two and three level cavities were formed, respectively, by performing one and two anodization–irradiation–dissolution sequences on the first level cavities. Only one or two grooves of the pattern were treated in this way for each experiment in order to save time. The results of the numerical simulations were used to precisely set the dissolution charge for a given experiment aimed at obtaining a specific cavity shape. After etching, the microstructured titanium disks were cut perpendicular to the grooves using a diamond saw. They were embedded in resin and mechanically polished with a 1 μm diamond finish. The cross sections of the grooves were then observed by optical microscopy. Figure 4 presents cross sections of four different cavity shapes. A single step cavity produced by etching of a flat surface is shown in Figure 4(a). The etching time of about 10 min produced a cavity of hemicylindrical shape of 40 μm diameter. This type of cavity served as a starting point for producing two level cavities. Figure 4(b,c,d) represent cavities produced by performing a second oxidation–irradiation–dissolution sequence on the original 40 μm groove. The dissolution time was 4, 17 and 75 min, respectively. The observed shapes correspond well to those predicted by the numerical simulations shown in Figure 3. A more quantitative comparison of the experimental and calculated shapes for a given charge was not attempted because of a lack of precise knowledge of the irradiated surface and the sample geometry used, but the order of magnitude of the experimental and theoretical volumes of dissolved material agreed well. The cavity of Figure 4(d) is slightly asymmetrical. This is attributed to an imperfect alignment of the second level laser trace in this experiment. Indeed, other experiments such as those shown in Figure 4 did not show such an asymmetry. The cavity of Figure 4(d) exhibits a shape with an opening smaller than the inner diameter in agreement with the numerical calculation for long dissolution times (Figure 3(b)).

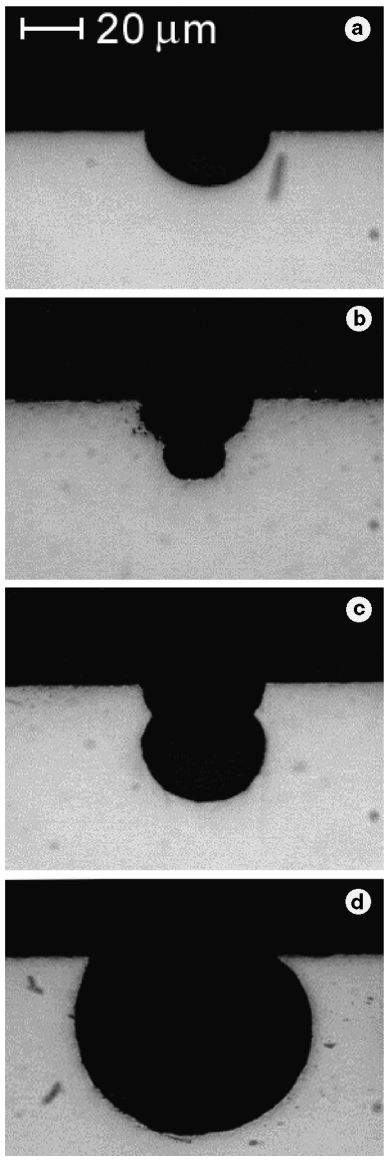

Fig. 4. (a) Cross section of electrochemically etched one level groove in titanium using oxide film laser lithography. (b–d) Cross sections of electrochemically etched two-level grooves at different dissolution times of 4, 17 and 35 min, respectively.

Figure 5 illustrates the shape of three-level cavities. They were produced from an initial two-level cavity shown in Figure 5(a), the centre of which was sensitized by laser irradiation. The cavity shapes resulting from the application of the third irradiation–anodization–dissolution sequence are shown in Figure 5(b,c,d) for different dissolution times (applied charge). After 16 min of anodic dissolution a well defined three-level cavity is obtained (Figure 5(b)). Its aspect ratio (AR) defined as the ratio depth/opening radius has a value of $AR \simeq 2.7$, more than twice the value of a hemispherical single step cavity ($AR \simeq 1$). With increasing dissolution time (67 min) the third level cavity enlarges and the shape

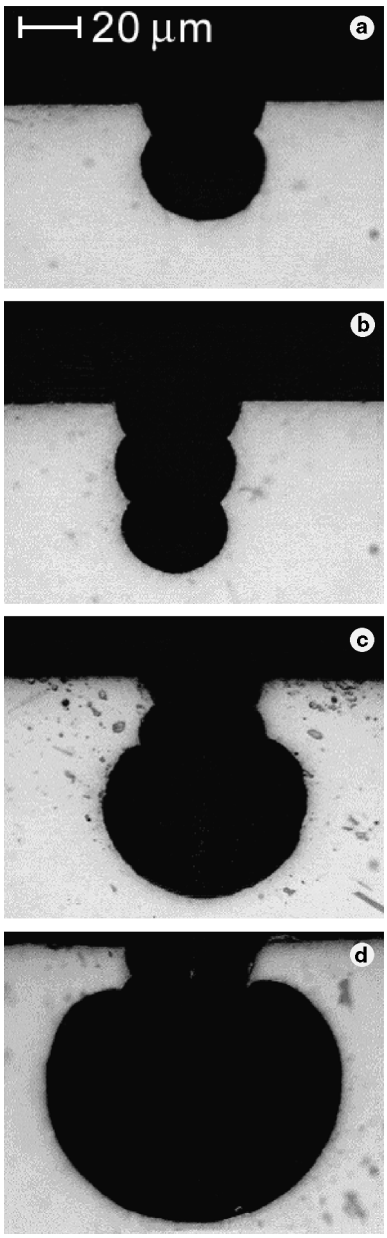

Fig. 5. (a) Cross section of electrochemically etched two-level groove in titanium serving for fabricating the three-level grooves shown in (b, c). Dissolution times are 16 min (b), 67 min (c) and 200 min (d), respectively.

evolves towards that of a deep cavity of relatively large diameter with a narrow neck. After 200 min dissolution (Figure 5(d)) the second level cavity is no longer visible. An amphora shaped large cavity with an inner diameter of more than 100 μm is formed. Its neck of about 35 μm diameter is much smaller than the cavity diameter. The experimentally observed shapes of the three level cavities of Figure 5 correspond well to those predicted by the numerical simulation (Figure 3(c)).

5. Discussion

The experimentally observed cavity shapes agree surprisingly well with those predicted by numerical simulations based on simple diffusion theory. This suggests that the assumptions made in the model were physically realistic. It has been shown previously that anodic dissolution of titanium in sulfuric acid–methanol electropolishing electrolytes is mass transport controlled and proceeds under limiting current conditions [11]. The transport limiting process involves diffusion of reaction products (dissolved tetravalent titanium species) from the anode surface towards the bulk electrolyte. The surface concentration of the diffusing species at the anode at the limiting current is equal to the saturation concentration. Madore et al. [6] found that the shape of single step cavities formed by electrochemical etching through a photo resist mask in the present electrolyte corresponded well to that calculated for a diffusion controlled process; convection did not have a significant effect. The cavity size in that study was comparable to that used here. It can therefore be reasonably concluded that for the present experimental conditions convection effects in the cavity were negligible.

In the present experiments an oxide film rather than a photoresist served to protect the nondissolving surface. The theoretical simulations assume that the protecting film stays in place during the dissolution process in spite of the fact that undercutting occurs. This means that the free standing thin oxide film should not deform or break off during an experiment, nor should it dissolve (cf. Figure 2). The fact that the experimentally observed and the calculated cavity shapes corresponded well indicates that the anodic oxide film indeed did neither break off nor significantly deform during dissolution. Ultrasound was used to remove the free standing oxide film after the experiments, and this permitted to neatly break off the films at the edge of the cavities.

A critical factor for cavity shape in a multistep process concerns the precision of the alignment of the laser beam used for oxide sensitization. The precision of alignment of the optical system used was in the micrometer range. This was sufficient for the present study; more precise alignment systems are available in the semiconductor industry and could be used for applications requiring a higher precision. A slight misalignment is thought to be responsible for the asymmetry observed in Figure 4(d), but in most cases the laser trace was located well in the centre of the grooves. The laser irradiation of the oxide film does not just lead to local ablation of the film, but involves several physical phenomena, which depend on the energy applied to the sample. The interactions between the laser beam and the titanium oxide films will be discussed in [27]. The irradiation conditions given in the experimental section were chosen to give best results for the present application.

From a micromachining point of view, the results of the present study demonstrate the feasibility of achieving unusual cavity shapes by multistep isotropic etching. This includes aspect ratios of two and more and amphora-like shapes with an inner radius larger than the neck. To the authors knowledge this is the first time that such shapes have been produced by isotropic

electrochemical etching. Furthermore, the results show that for systems exhibiting mass transport controlled dissolution, the shape evolution with applied charge can be predicted by numerical simulation for different starting geometries. Using numerical simulation as a tool increases greatly the design flexibility and thus can open new applications. From a practical point of view, producing multilevel cavities using OFLL is quite time consuming and requires precise sample positioning for subsequent irradiations. However, it is possible to carry out the electrochemical dissolution simultaneously on many cavities and, in principle, a splitted laser beam could be used for simultaneously creating many features of a pattern. By addressing such problems, the practical usefulness of OFLL electrochemical micromachining of multilevel cavities could be greatly enhanced.

From the point of view of localized corrosion, the present results can shed new light on the shape evolution of growing corrosion pits. It has been shown previously that the results of 2D shape change simulations representing the cross section of a cylindrical groove do not differ substantially from those obtained for spherical geometries typical for corrosion pits [2, 6]. Also, it is well known that under certain conditions the growth of corrosion pits is diffusion controlled (salt film mechanism) [16–18, 20, 22, 24, 25]. According to this mechanism, the rate of metal dissolution in the pit is governed by the rate of mass transport of the metal ions away from the salt film covered anode surface and the surface concentration corresponds to the saturation concentration. This is the same mechanism, which holds for cavity growth in the present model system, namely anodic dissolution of titanium in sulfuric acid–methanol electropolishing solution [6, 11]. Corrosion pits formed under mass transport control would therefore be expected to exhibit similar shapes as found in electrochemical micromachining. Indeed, several authors have reported hemispherical pit shapes formed under anodic polarisation conditions, which lead to salt film formation [15, 22]. More often, however, pit shapes are more complicated and pits are partly occluded. Laycock and White studied the formation of occluded pits on stainless steel in chloride solution [25]. They found that dissolution leads to undercutting and formation of a covered pit. These authors proposed a qualitative model for pit growth assuming that growth starts from a hemispherical nucleus. Repassivation at the edges would lead to undercutting and formation of a lacy cover. Recently, Laycock and coworkers [20, 24] proposed mathematical models of pit growth based on these concepts. The authors considered nonsteady state diffusion and the kinetics of the dissolution reaction on an expanding pit surface as well as repassivation conditions. Wang et al. [21] explained the shape of pits with a neck by a model in which the *IR* drop in the solution permits passivation of the cavity neck.

The mass transport model proposed in the present paper is much simpler. It considers pseudo steady state conditions and transport controlled dissolution through a mask. Its effectiveness in describing the observed multilevel cavity shapes is all the more astonishing. Apparently, under the present experimental conditions neither *IR* drops nor interfacial kinetics played a significant role for pit growth. It is intriguing to speculate whether similar considerations could apply for pit formation under corrosion conditions. It is generally recognised that depassivation and repassivation phenomena occur during pit initiation and it can not be excluded that similar phenomena may also take place during pit growth under certain conditions. Indeed, a close observation of the bottom of large pits sometimes indicates the presence of small 'pits-in-a-pit' suggesting that passivation and pit initiation processes occurred during growth. Initiation of a new pit at the bottom of an existing (repassivated) pit could have a drastic effect on the shape evolution under diffusion controlled growth conditions. Deeper pits and amphora-like pit shapes become thus theoretically possible. Mass transport controlled pit growth therefore does not necessarily lead to hemispherical pit shapes.

6. Conclusions

Using oxide film laser lithography multilevel cavities have been produced by isotropic electrochemical etching of titanium in an electropolishing electrolyte applying up to three oxidation–irradiation–anodic dissolution steps.

Theoretical simulations showed that isotropic etching involving two or more dissolution steps can yield cavities with a high aspect ratio or deep cavities with a neck.

The shapes of two-level and three-level cavities formed on titanium by diffusion controlled anodic dissolution through oxide film masks corresponded well to those predicted by numerical simulation.

The present results suggest that local depassivation events at the bottom of a passive cavity can have a drastic effect on its shape evolution under diffusion controlled growth conditions.

Acknowledgements

This study was financially supported by Fonds national Suisse pour la recherche scientifique in Bern, Switzerland. The authors thank Professor Alan West of Columbia Univeristy (New York) for providing them with the LAPLACE computer code and Dr Patrik Hoffmann for access to the laser set-up.

References

1. E. Rosset and D. Landolt, *Precision Eng.* **11** (1989) 79.
2. A.C. West, C. Madore, M. Matlosz and D. Landolt, *J. Electrochem. Soc.* **139** (1992) 499.
3. M. Datta and L.T. Romankiw, *J. Electrochem. Soc.* **136** (1989) 285C.

4. C. Madore and D. Landolt, *J. Micromech. Microeng.* **7** (1997) 270.
5. M. Datta and D. Harris, *Electrochim. Acta* **42** (1997) 3007.
6. C. Madore, O. Piotrowski and D. Landolt, *J. Electrochem. Soc.* **146** (1999) 2526.
7. M. Datta and D. Landolt, *Electrochim. Acta* **45** (2000) 2535.
8. Y. Ferri, O. Pietrowski, P.F. Chauvy, C. Madore and D. Landolt, *J. Micromech. Microeng.* **11** (2001) 522.
9. R.V. Shenoy and M. Datta, *J. Electrochem. Soc.* **143** (1996) 544.
10. R.V. Shenoy, M. Datta and L.T. Romankiw, *J. Electrochem. Soc.* **143** (1996) 2305.
11. O. Piotrowski, C. Madore and D. Landolt, *J. Electrochem. Soc.* **145** (1998) 2362.
12. P-F. Chauvy, C. Madore and D. Landolt, *Electrochem. Solid State Lett.* **2** (1999) 123.
13. P-F. Chauvy, P. Hoffmann and D. Landolt, *Electrochem. Solid State Lett.* **4** (2001) C31.
14. P-F. Chauvy, P. Hoffmann and D. Landolt, *Appl. Surf. Sci.*, submitted.
15. K.J. Vetter and H.H. Strehblow, *in* R.W. Staehle, B.F. Brown, J. Kruger and A. Agarwal (Eds), 'Localized Corrosion', NACE-3, NACE, Houston, TX (1974), p. 240.
16. H.H. Strehblow and J. Wenners, *Z. Phys. Chem. (N. F.)* **98** (1975) 199.
17. H.C. Kuo and D. Landolt, *Corros. Sci.* **16** (1976) 915.
18. F. Hunkeler, A. Krolikowski and H. Böhni, *Electrochim. Acta* **32** (1987) 615.
19. R.C. Alkire and K.P. Wong, *Corros. Sci.* **28** (1988) 411.
20. P. Ernst, N.J. Laycock, M.H. Moayed and R.C. Newman, *Corros. Sci.* **39** (1997) 1133.
21. M.Wang, H.W. Pickering and Y. Xu, *J. Electrochem. Soc.* **142** (1995) 2986.
22. P. Ernst and R.C. Newman, *Corros. Sci.* **44** (2002) 927.
23. P. Ernst and R.C. Newman, *Corros. Sci.* **44** (2002) 943.
24. N.J. Laycock, S.P. White, J.S. Noh, P.T.Wilson and R.C. Newman, *J. Electrochem. Soc.* **145** (1998) 1101.
25. N.J. Laycock and S.P. White, *J. Electrochem. Soc.* **148** (2001) B264.
26. P-F. Chauvy, 'Electrochemical Micromachining of Titanium using Oxide Film Laser Lithography', PhD. thesis no. 2570, EPFL, Lausanne (2002).
27. P-F. Chauvy, P. Hoffmann and D. Landolt, *Appl. Surf. Sci.* submitted.